JOURNAL OF GUIDANCE, CONTROL, AND DYNAMICS
Vol. 35, No. 4, July–August 2012

Magnetic Detumbling of a Rigid Spacecraft

Giulio Avanzini*
University of Salento, 72100 Brindisi, Italy
and
Fabrizio Giulietti†
University of Bologna, 47100 Forlì, Italy

DOI: 10.2514/1.53074

In this paper, a control law that detumbles a spacecraft with magnetic actuators only is developed. A rigorous mathematical proof of global asymptotic convergence from arbitrary initial tumbling conditions to zero angular velocity in a time-varying magnetic field is derived. Furthermore, a simple criterion for determining a reasonable value of the control gain is developed. The selected gain results in a quasi-minimum time detumbling for different initial conditions, in the presence of magnetic coil saturation. Performance of the proposed detumbling control law is demonstrated by numerical simulations on a large set of test cases using a Monte Carlo approach.

I. Introduction

TOGETHER with active attitude stabilization and disturbance rejection, the attitude control system (ACS) detumbles a spacecraft immediately after launch. Detumbling consists of damping all angular velocity components of the spacecraft to zero. Either thrusters or magnetic coils may be used [1]. In a fully actuated system using thrusters, three-axis control is available and detumbling is rather straightforward. In such a case, it is easy to prove that the kinetic energy $\mathcal{T}$ of the spacecraft steadily decreases for a control torque defined as $\boldsymbol{M}_c = -k\boldsymbol{\omega}$, such that $\boldsymbol{\omega} \to 0$ as $t \to \infty$; that is, a rest condition is asymptotically achieved [2]. Practical problems arise when detumbling is to be achieved in a finite time in the presence of a limited control effort. Several control techniques have been developed that take into account these practical problems, such as the time-optimal controller proposed by Aghili [3] or the elegant analytical solution derived by Romano for axially symmetric spacecraft [4]. All these approaches require that the spacecraft is fully actuated.

If the spacecraft is underactuated (i.e., only two control torque components are available for controlling three rotational degrees of freedom), every attitude control task, including detumbling, becomes significantly more difficult [5]. When magnetic torquers only are employed as attitude effectors for satellites on inclined low Earth orbits (LEOs), the resulting ACS is inherently underactuated. This is the only (yet major) drawback for this class of actuators. In every other respect, magnetic torquers are characterized by many interesting properties [6], such as 1) the absence of catastrophic failure modes; 2) a virtually unlimited operational life, because of their simple and reliable architecture and the need for renewable electrical power only to operate them; 3) the possibility of smoothly modulating the control torque, which does not induce unwanted coupling with flexible modes, as it occurs with thrusters [7]; and 4) significant savings in overall system weight and complexity with respect to any other class of actuators, as there are no moving parts or plumbing.

These features motivate the strong interest in magnetic actuators since they were first proposed almost 50 years ago [8], although a different type of actuator usually accompanies the magnetics to provide full three-axis control. In many cases, an ACS based on a combination of reaction wheels or momentum-bias wheels is adopted for accurate pointing, whereas magnetic coils are installed for angular momentum dumping tasks (detumbling and wheel desaturation) [9]. Only more recently, fully magnetic attitude control was considered as a viable option, especially interesting for low-cost microsatellites or for control system reconfiguration after failure. In this latter framework, the works by Lovera and Astolfi demonstrated the possibility of achieving adequate pointing precision by means of a fully magnetic system [10,11].

In the present paper, a rigorous proof of global asymptotic stability is derived for detumbling performed by magnetic actuators, where the angular velocity components are driven to zero asymptotically by means of a static linear feedback. The task is simpler than that considered by Lovera and Astolfi, but the proposed solution is based on a novel lemma of general validity derived from a corollary to Barbalat's lemma [12]. The new lemma is applicable to all those nonautonomous systems that feature a time-invariant candidate Lyapunov function, under conditions that will be outlined in Sec. II.

The proposed command law represents an alternative version of the well-known B-dot control law [6]. The proof demonstrates that, in the presence of a time-varying magnetic field, the kinetic energy is strictly decreasing, which means that it approaches zero monotonically. This is a stronger property than what Stickler and Alfriend demonstrated, proving that the time derivative of the kinetic energy is $\dot{\mathcal{T}} \leq 0$, but showing only empirically that the residual motion about the direction of the magnetic field is almost canceled by their command law with the rotation of the magnetic field over time with respect to the orbital frame.

As a further contribution, the novel framework allows for a physical interpretation of the mechanism at the basis of the asymptotic convergence obtained by means of the considered angular rate feedback. The critical parameter to keep under control is the angular distance between the direction of the magnetic field and the angular velocity vector. This angle should not be allowed to be zero, in order to maintain a nonzero control power along the instantaneous axis of rotation of the spinning motion. Following this interpretation, it is possible to derive a simple yet effective way of sizing the feedback control law gain that performs detumbling in a relatively short duration. At the same time, a smooth feedback control law avoids possible excitation of flexible modes caused by bang–bang techniques, like that proposed in [13] that, by abruptly changing the direction of the control torques, induces discontinuous variations of the angular acceleration.

In what follows, the new lemma is derived in Sec. II, which provides sufficient conditions for global asymptotic stability of

Received 8 November 2010; revision received 17 December 2011; accepted for publication 19 December 2011.

*Professor, Faculty of Industrial Engineering, Cittadella della Ricerca, S.S. 7 km 7 + 300; giulio.avanzini@unisalento.it. Senior Member AIAA.

†Assistant Professor, Department of Mechanical and Aerospace Engineering (DIEM), Via Fontanelle 40; fabrizio.giulietti@unibo.it. Senior Member AIAA.

nonautonomous systems featuring a negative semidefinite derivative of a time-invariant Lyapunov-like function. In Sec. III, after formulating the detumbling problem for a rigid spacecraft, the proposed control law is introduced and its convergence to zero angular velocity is proved on the basis of the new lemma. Section III ends with the derivation of the control law gain that provides quasi-optimal performance in terms of convergence time. In Sec. IV, the resulting closed-loop behavior for different values of the gain is analyzed by means of numerical simulation. A Monte Carlo approach is adopted in order to prove that the gain chosen according to the technique developed in the present paper results in convergence to a rest condition in minimum time, on the average. Section V concludes the paper.

II. Preliminary Result

The proof of asymptotic stability of the control law developed in the next section is based on a novel lemma obtained by extending the application of a corollary of Barbalat's lemma, known as the Lyapunov-like lemma (see [12], p. 125), to nonautonomous dynamical systems featuring Lyapunov-like functions independent of time. The Lyapunov-like lemma is as follows:

Lemma 1: If a scalar function $V(\boldsymbol{x}, t)$ satisfies the following conditions, where 1) $V(\boldsymbol{x}, t)$ is lower bounded, 2) $\dot{V}(\boldsymbol{x}, t)$ is negative semidefinite, and 3) $\dot{V}(\boldsymbol{x}, t)$ is uniformly continuous in time, then $\dot{V}(\boldsymbol{x}, t) \to 0$ as $t \to \infty$.

From this result, it is possible to derive the following:

Lemma 2: Consider a nonlinear nonautonomous dynamic system

$$\dot{\boldsymbol{x}} = \boldsymbol{f}(\boldsymbol{x}, t) \tag{1}$$

where $\boldsymbol{f}$: $\mathbb{R}^n \times \mathbb{R} \to \mathbb{R}^n$ is a smooth time-dependent vector field, featuring at least one equilibrium at the origin. Also assume that a strictly positive definite Lyapunov-like function

$$V(\boldsymbol{x}) > 0$$

exists, where 1) V: $\mathbb{R}^n \to \mathbb{R}$ is a smooth scalar function of the state $\boldsymbol{x}$ only and 2) its gradient vanishes at the origin only; that is, $\nabla_x V = \boldsymbol{0}$ at $\boldsymbol{x} = \boldsymbol{0}$ and $\nabla_x V \neq \boldsymbol{0}$ elsewhere.

If the Lyapunov-like function $V(\boldsymbol{x})$ and its time derivative $\dot{V}$ satisfy the following conditions, 1) $\dot{V}$ is negative semidefinite (that is, $\dot{V}[\boldsymbol{x}(t)] \leq 0$), 2) $\dot{V}$ is uniformly continuous, and 3) the isosurfaces S of $V(\boldsymbol{x})$ in the state space $\mathbb{R}^n$ do not contain any integral curves $\boldsymbol{x}(t)$ of the vector field $\boldsymbol{f}$ other than the constant ones ($\boldsymbol{x}(t) = \boldsymbol{x}_e$, $\forall\ t$), then the state converges to one of the (at least locally) stable equilibria. If the origin is the only equilibrium, it is globally asymptotically stable.

Proof: The Lyapunov-like lemma ensures that, under the above assumptions,

$$\lim_{t\to\infty} \dot{V}(\boldsymbol{x}, t) = 0$$

This implies that the lower-bounded Lyapunov-like function V asymptotically approaches a steady-state value V_∞:

$$\lim_{t\to\infty} V(\boldsymbol{x}) = V_\infty$$

where any value $V_\infty \neq 0$ means that the equilibrium at the origin is not reached. The time derivative of V is given by

$$\dot{V} = \frac{\mathrm{d}V}{\mathrm{d}t} = \frac{\partial V}{\partial \boldsymbol{x}}\frac{\mathrm{d}\boldsymbol{x}}{\mathrm{d}t} = \nabla_x V \cdot \boldsymbol{f}$$

and it vanishes if one of the following three conditions is (asymptotically) approached:

1) The vector field vanishes; that is, $\boldsymbol{f} \to \boldsymbol{0}$, in which case an equilibrium is approached and the lemma is satisfied.

2) The gradient of V vanishes; that is, $\nabla_x V \to \boldsymbol{0}$, but this is possible only if the origin is reached, under assumption 2 on V, where an equilibrium for the system is postulated and the lemma is again satisfied.

3) The gradient of V becomes perpendicular to the vector field $\boldsymbol{f}$.

In case 3, the solution $\boldsymbol{x}(t)$ converges to an isosurface S_∞ such that $V(\boldsymbol{x}) = V_\infty$, with $\boldsymbol{f} \neq \boldsymbol{0}$. Under the assumed continuity properties of both the Lyapunov-like function V and the vector field $\boldsymbol{f}$, S_∞ must contain at least one attractive integral curve $(\boldsymbol{x}(t), t)$ of the vector field $\boldsymbol{f}$ that is asymptotically approached,but it is not an equilibrium, and this is in contradiction with the last assumption of the lemma.

Then, condition 3 cannot be reached and only condition 1 or 2 can be satisfied; that is, one of the equilibria is asymptotically approached and Lemma 2 is proved. If the origin is the only equilibrium, it will be asymptotically reached from any initial condition.

Remark 1: Stated in other words, the last assumption of Lemma 2 requires that no solutions of the system of ordinary differential equation [Eq. (1)] lie on the isosurfaces S, other than the equilibria. In this latter case, the value of $V(\boldsymbol{x}_e)$ associated with an equilibrium $\boldsymbol{x}_e$ is necessarily constant in time so that, once a steady state $\boldsymbol{x}_e$ is approached, $V \to V(\boldsymbol{x}_e) = V_\infty$ and $\dot{V} \to 0$, as required by Barbalat's lemma. So, if the equilibrium set R of Eq. (1) contains solutions other than the origin, it is not possible to state a priori which one will be reached, yet the lemma guarantees that, under the conditions stated in Lemma 2, sooner or later an equilibrium will be approached.

Remark 2: In the most general case, it may not be trivial to prove that the isosurfaces $S = \{\boldsymbol{x} | V(\boldsymbol{x}) = k, k > 0\}$ of the candidate Lyapunov-like function V contain no solutions of the vector field $\boldsymbol{f}$, other than the equilibrium set R. This is particularly true when a general solution for Eq. (1) is not available and/or it is not possible to derive an explicit equation for S from its implicit definition. But this task is easier in all those cases when the derivative of the Lyapunov-like function is expressed in a simple form, e.g., by means of a negative semidefinite quadratic form:

$$\dot{V}(\boldsymbol{x}, t) = -\boldsymbol{x}^T \boldsymbol{\Phi}(t) \boldsymbol{x} \tag{2}$$

In this situation, the proof that $\dot{V}$ is uniformly continuous, as required by Lemma 1, usually becomes straightforward.

III. Problem Statement and Solution

A. System Dynamics

The dynamic model of a rigid satellite expressed in a set of principal axes of inertia, $\mathbb{F}_B = \{P; \hat{\boldsymbol{e}}_1, \hat{\boldsymbol{e}}_2, \hat{\boldsymbol{e}}_3\}$, centered in the spacecraft center of mass P is given by Euler equations

$$\boldsymbol{I}\,\dot{\boldsymbol{\omega}} = \boldsymbol{M} - \boldsymbol{\omega} \times (\boldsymbol{I}\boldsymbol{\omega}) \tag{3}$$

where $\boldsymbol{\omega} = (\omega_1, \omega_2, \omega_3)^T$ is the absolute angular velocity vector with respect to an inertial frame $\mathbb{F}_I$, $\boldsymbol{I} = \mathrm{diag}(J_1, J_2, J_3)$ is the spacecraft inertia matrix, and $\boldsymbol{M} = (M_1, M_2, M_3)^T$ is the external torque. Since no external disturbance is considered in the present analysis, $\boldsymbol{M}$ represents the control torque delivered by the magnetic coils.

For spacecraft controlled by means of three orthogonal magnetic coils, the torque generated by the magnetorquers can be modeled as

$$\boldsymbol{M} = \boldsymbol{m} \times \boldsymbol{b} \tag{4}$$

where $\boldsymbol{m} = (m_1, m_2, m_3)^T$ is the commanded magnetic dipole moment vector generated by the coils and $\boldsymbol{b} = (b_1, b_2, b_3)^T$ is the local geomagnetic field vector expressed in terms of body-frame components.

The Earth geomagnetic field can be approximated by a tilted magnetic dipole of moment $M_\oplus = 7.8379 \times 10^6$ T km^3, with a tilt angle of $\gamma_m = 11.44$ deg with respect to the polar axis [1]. Consider now a local-horizontal/local-vertical orbit frame $\mathbb{F}_O$, where the z_O axis lies along the local vertical; the y_O axis is normal to the orbit plane, in a direction opposite to the orbital angular speed $\boldsymbol{\omega}^{\mathrm{orb}}$; and the transverse axis x_O completes a right-handed triad, in the direction of the orbital velocity (Fig. 1). For a circular LEO of radius r_c, the components of the geomagnetic vector can be expressed in $\mathbb{F}_O$ as [14]

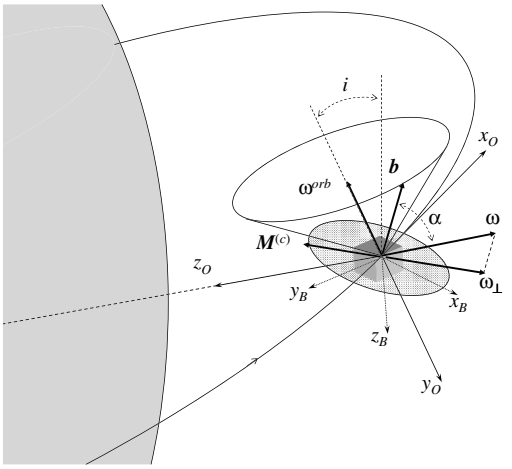

Fig. 1 Geometry of the problem.

$$\boldsymbol{b}_O = \frac{M_\oplus}{r_c^3}\begin{bmatrix} \sin\xi_m \cos(\Omega t - \eta_m) \\ -\cos\xi_m \\ 2\sin\xi_m \sin(\Omega t - \eta_m) \end{bmatrix} \tag{5}$$

where

$$\cos\xi_m = \cos i \cos\gamma_m + \sin i \sin\gamma_m \cos\beta'_m$$
$$\sin\eta_m \sin\xi_m = -\sin\gamma_m \sin\beta'_m$$
$$\cos\eta_m \sin\xi_m = \sin i \cos\gamma_m - \cos i \sin\gamma_m \cos\beta'_m$$
$$\beta'_m = \beta_m + \omega_e t - \Omega_{\text{an}}$$

i is orbit inclination, $\Omega = 2\pi/T_{\text{orb}}$ is the orbit rate, ω_e is the Earth angular rate, Ω_{an} is the ascending node of the spacecraft orbit, and β_m is the initial value of the angle between the vernal equinox and the line of intersection of the equatorial plane with the geomagnetic equator. The angle ξ_m represents the inclination of the spacecraft orbit relative to the geomagnetic equatorial plane, and η_m is the angle between the ascending node relative to the Earth's equator and the ascending node relative to the geomagnetic equator.

The components of the Earth magnetic field in $\mathbb{F}_B$ are $\boldsymbol{b} = \mathbb{T}_{BO}\boldsymbol{b}_O$, where

$$\mathbb{T}_{BO} = (q_0^2 - \boldsymbol{q}^T\boldsymbol{q})\mathbb{I}_3 + 2\boldsymbol{q}\boldsymbol{q}^T - 2\bar{q}\,\tilde{\mathbb{Q}}$$

is the coordinate transformation matrix between $\mathbb{F}_O$ and $\mathbb{F}_B$. In the latter formula, $\boldsymbol{Q} = (\boldsymbol{q}^T, \bar{q})^T$ is the unit quaternion that represents spacecraft attitude with respect to $\mathbb{F}_O$, $\mathbb{I}_3$ is a 3×3 identity matrix, and $\tilde{\mathbb{Q}}$ is the skew-symmetric matrix equivalent of the cross product, such that $\tilde{\mathbb{Q}}\boldsymbol{v} = \boldsymbol{q} \times \boldsymbol{v}$ for any $\boldsymbol{v} \in \mathbb{R}^3$. The evolution of $\boldsymbol{Q}$ is given by [2]

$$\dot{\boldsymbol{q}} = \tfrac{1}{2}(\bar{q}\boldsymbol{\omega}^r - \boldsymbol{\omega}^r \times \boldsymbol{q}) \qquad \dot{\bar{q}} = -\tfrac{1}{2}\boldsymbol{\omega}^{rT}\boldsymbol{q} \tag{6}$$

where

$$\boldsymbol{\omega}^r = \boldsymbol{\omega} - \mathbb{T}_{BO}\boldsymbol{\omega}_O^{\text{orb}} \tag{7}$$

is the angular speed of the spacecraft relative to $\mathbb{F}_O$, whereas $\boldsymbol{\omega}_O^{\text{orb}} = (0, -\Omega, 0)^T$ is the angular speed of $\mathbb{F}_O$ with respect to an inertial frame.

B. Detumbling Control Law

The objective of this section is to design an efficient control law that reduces the angular rates to zero from arbitrary initial values (e.g., random angular velocity components, after release from the payload bay of a rocket launcher). This needs to be done in a reasonably short amount of time and with limited current levels in the magnetic coils in order to reduce battery consumption. To this aim, the following control law is analyzed:

$$\boldsymbol{M} = -k_\omega(\mathbb{I}_3 - \hat{\boldsymbol{b}}\hat{\boldsymbol{b}}^T)\boldsymbol{\omega} \tag{8}$$

where $\hat{\boldsymbol{b}} = \boldsymbol{b}/\|\boldsymbol{b}\|$ is the unit vector parallel to the local geomagnetic vector, expressed in terms of body-frame components, and the resulting control torque is clearly perpendicular to $\hat{\boldsymbol{b}}$. This feedback law is similar to that proposed by Markley [15]. As a minor difference, a linear control law is used here, instead of the switching control logic discussed in [15]. A criterion for the choice of the gain will be discussed in the next section.

To use the Lyapunov stability theorems, the rotational kinetic energy is chosen as the strictly positive definite candidate Lyapunov function:

$$V = \tfrac{1}{2}\boldsymbol{\omega}^T\boldsymbol{I}\boldsymbol{\omega} \tag{9}$$

Its time derivative is $\dot{V} = \boldsymbol{\omega}^T\boldsymbol{M}$. By substituting Eq. (8), one has

$$\dot{V} = -k_\omega\boldsymbol{\omega}^T(\mathbb{I}_3 - \hat{\boldsymbol{b}}\hat{\boldsymbol{b}}^T)\boldsymbol{\omega} \tag{10}$$

Note that, in the present case, $\dot{V}$ is expressed by means of a quadratic form, as indicated in Eq. (2), where $\boldsymbol{\Phi}(t)$ is the time-dependent matrix

$$\boldsymbol{\Phi}(t) = k_\omega(\mathbb{I}_3 - \hat{\boldsymbol{b}}\hat{\boldsymbol{b}}^T)$$

It is easy to show that $\dot{V}$ is only negative semidefinite, inasmuch as $\dot{V}$ vanishes not only when $\boldsymbol{\omega} \to \boldsymbol{0}$, but also whenever $\boldsymbol{\omega}$ becomes parallel to $\boldsymbol{b}$. This situation needs thus be avoided: when the spacecraft rotates exactly about an axis parallel to the direction of the local geomagnetic field, the magnetic coils cannot deliver any torque component about the current spin axis in order to further decrease the angular speed. This condition is maintained when one of the principal axes of inertia converges onto the geomagnetic field so that no precession motion is present and a pure spin condition about $\hat{\boldsymbol{e}}_i \equiv \hat{\boldsymbol{b}}$ is achieved. This is what happens when the control law given by Eq. (8) is applied for a time-invariant direction of the vector $\hat{\boldsymbol{b}}_O$, as will be shown in Sec. IV. In practical situations, such a condition is never met and a proof of asymptotic stability can be derived.

C. Asymptotic Stability for the Detumbling Maneuver

To apply the new corollary of the Lyapunov-like lemma to the present case, it is necessary to prove that $\dot{V}$, expressed by Eq. (10), satisfies requirements 1, 2, and 3 of Lemma 2. The first requirement (that is, $\dot{V}$ is negative semidefinite) is trivially proved from Eq. (10), as shown above.

Requirement 2 (that is, uniform continuity of $\dot{V}$) can be proved considering that, for any real valued function $f(x)$, a sufficient condition for uniform continuity is that f is Lipschitz-continuous of degree α. This means that there exists a finite positive constant $c > 0$ such that $|f(y) - f(x)| \le c|y - x|^\alpha$. A sufficient condition for Lipschitz continuity of degree $\alpha = 1$ is that the derivative $f'(x) = \mathrm{d}f/\mathrm{d}x$ is bounded. To demonstrate uniform continuity of $\dot{V}$, it is thus sufficient to prove that $\ddot{V}$ is bounded, which easily follows from the absence of impulsive control torques.

Lemma 2 can thus be applied if one demonstrates also that the third condition holds. In the most general case, Eq. (10) shows that $\dot{V} = 0$ if $\boldsymbol{\omega} \in \ker(\boldsymbol{\Phi})$, i.e., if the angular velocity vector $\boldsymbol{\omega}$ is parallel to the direction $\hat{\boldsymbol{b}}$ of the magnetic field, in which case the angular velocity can be expressed in the form $\boldsymbol{\omega} = \omega\hat{\boldsymbol{b}}$, where $\omega = \|\boldsymbol{\omega}\|$. The resulting control torque in this situation would be $\boldsymbol{M} = -k_\omega\omega(\mathbb{I}_3 - \hat{\boldsymbol{b}}\hat{\boldsymbol{b}}^T)\hat{\boldsymbol{b}} = \boldsymbol{0}$.

Considering the closed-loop system obtained by substituting Eq. (8) into Eq. (3),

$$\dot{\boldsymbol{\omega}} = -\boldsymbol{I}^{-1}[k_\omega(\mathbb{I}_3 - \hat{\boldsymbol{b}}\hat{\boldsymbol{b}}^T)\boldsymbol{\omega} + \boldsymbol{\omega} \times (\boldsymbol{I}\boldsymbol{\omega})] \tag{11}$$

requirement 3 thus holds if the inequality

$$\boldsymbol{I}\,(\dot{\omega}\,\hat{\boldsymbol{b}} + \omega\dot{\hat{\boldsymbol{b}}}) \neq -\omega^2[\hat{\boldsymbol{b}} \times (\boldsymbol{I}\hat{\boldsymbol{b}})] \tag{12}$$

holds for the considered variation of Earth's magnetic field. This is easily proven by considering the evolution of the angular velocity vector in the inertial space for the torque-free case, showing that the direction of $\boldsymbol{\omega}$ cannot follow the direction of the Earth magnetic field $\boldsymbol{b}$. Three cases are possible [2]: 1) spherically symmetric mass distribution ($J_1 = J_2 = J_3$); 2) axially symmetric spacecraft ($J_1 = J_2 \neq J_3$); and 3) tri-inertial satellites (with three different principal moments of inertia).

When no torque is applied, the angular momentum vector $\boldsymbol{h}$ of the spacecraft remains constant in the inertial space. If the principal moments of inertia are all equal, the direction of $\boldsymbol{\omega}$ is parallel to the (inertially fixed) direction of $\boldsymbol{h}$, and thus $\boldsymbol{\omega}$ cannot remain parallel to $\boldsymbol{b}$, which rotates in both the orbital and inertial frames. Moreover, the shape of the surface spanned by $\boldsymbol{b}$ is a slowly rotating elliptical cone, described by Eq. (5), that thus cannot match the shape of the circular space cone drawn by $\boldsymbol{\omega}$ around $\boldsymbol{h}$ in the axisymmetric case [2]. A direction of $\boldsymbol{\omega}$ parallel to $\boldsymbol{b}$ cannot thus represent a physically feasible solution for the motion of an axially symmetric spacecraft.

A more complex situation is dealt with when one considers a tri-inertial satellite. In this case, the angular velocity vector for a torque-free motion draws a curve called a herpolhode, which in the most general case is open and characterized by a rather complex shape, clearly preventing $\boldsymbol{\omega}$ from tracking the direction of $\boldsymbol{b}$. When principal moments of inertia with integer ratios are considered, the herpolhode can become a closed curve, but its position is fixed in the inertial space. In the unlikely situation in which its shape becomes an ellipse with exactly the same size and shape of the trace of $\boldsymbol{b}$, Earth's rotation would slowly but unavoidably prevent this condition from being maintained in the long run. Moreover, the actual direction of the geomagnetic field follows a much more complex pattern than that described by the simple tilted dipole model here considered, especially for nonequatorial orbits, showing a large number of anomalies.

As a consequence, $\boldsymbol{\omega} = \omega\hat{\boldsymbol{b}}$ can never be a solution for the motion of a spinning spacecraft in the torque-free case. This proves that, for a time-varying direction of the magnetic field, the inequality in Eq. (12) holds and no equilibrium other than $\boldsymbol{\omega} = \boldsymbol{0}$ exists nor any other solution on isosurfaces $V = \text{const}$. In such a case, Lemma 2 provides a rigorous proof of global asymptotic stability toward the origin, when the control law expressed by Eq. (8) is applied to a rigid spacecraft.

Remark 3: Note that, if one disregards the orbital motion, assuming that $\|\boldsymbol{\omega}_O^{\text{orb}}\| \ll \|\boldsymbol{\omega}\|$ and $\dot{\hat{\boldsymbol{b}}}_O \approx \boldsymbol{0}$, the inequality is not verified. In such a case, it is possible to have $\dot{\omega}\boldsymbol{I}\hat{\boldsymbol{b}} = -\omega^2[\hat{\boldsymbol{b}} \times (\boldsymbol{I}\hat{\boldsymbol{b}})] = \boldsymbol{0}$ if one of the principal axes of inertia lies along the (approximately fixed) direction of the magnetic field and the spacecraft spins about that axis at constant angular speed ω. This means that, for a constant direction of the magnetic field in $\mathbb{F}_O$, it is not possible to detumble the spacecraft with the considered control law, as the spacecraft will usually converge toward a pure spin condition around one of the principal axes of inertia aligned with $\hat{\boldsymbol{b}}$.

D. Implementation of the Control Law

Since $\boldsymbol{M} = \boldsymbol{m} \times \boldsymbol{b}$, the internal dipole vector $\boldsymbol{m}$ that lies in the plane perpendicular to the Earth magnetic field generates the maximum control torque for a given value of the total internal dipole moment, i.e., for a given value of the current absorbed by the torque rods. No electricity is thus wasted in producing ineffective dipole components along $\hat{\boldsymbol{b}}$. By introducing the orthogonality condition between the vectors $\boldsymbol{m}$ and $\boldsymbol{b}$ (that is, $\boldsymbol{m}^T\hat{\boldsymbol{b}} = 0$), one gets

$$\boldsymbol{m} = \frac{1}{\|\boldsymbol{b}\|^2}(\boldsymbol{b} \times \boldsymbol{M}) = \frac{1}{\|\boldsymbol{b}\|}(\hat{\boldsymbol{b}} \times \boldsymbol{M}) \tag{13}$$

By taking into account the expression of the control torque $\boldsymbol{M}$ in Eq. (8), one finally gets

$$\boldsymbol{m} = -\frac{k_\omega}{\|\boldsymbol{b}\|}\hat{\boldsymbol{b}} \times [(\mathbb{I}_3 - \hat{\boldsymbol{b}}\hat{\boldsymbol{b}}^T)\boldsymbol{\omega}] = -\frac{k_\omega}{\|\boldsymbol{b}\|}(\hat{\boldsymbol{b}} \times \boldsymbol{\omega}) \propto \boldsymbol{\omega} \times \hat{\boldsymbol{b}} \tag{14}$$

The similarity with the so-called B-dot control law proposed by Stickler and Alfriend [6] and Markley [15] is evident, where the magnetic coil dipole moment command is defined as

$$\boldsymbol{m} \propto \boldsymbol{\omega} \times \boldsymbol{b} \approx -\dot{\boldsymbol{b}}$$

As a minor difference, note that the direction $\hat{\boldsymbol{b}}$ of the magnetic field rather than the magnetic field vector $\boldsymbol{b}$ itself is adopted in the definition of the command law in Eq. (14). More important, a rigorous proof of global asymptotic stability is now available, according to the derivation above, which provides theoretical support to the fundamental result proposed by Stickler and Alfriend more than 30 years ago [6]. As far as the practical implementation of the command law is concerned, an important difference lies in the fact that the B-dot feedback control law does not require a direct measurement or estimate of angular velocity components. This fact constitutes a clear advantage for small spacecraft equipped with magnetic actuators only, but such a configuration is still rather unusual. In most applications, attitude information (including angular velocity components) is usually available from onboard sensors, and the detumbling control law can be implemented as expressed in Eq. (14).

If no rate information is available, a modified version of the B-dot command law can be derived from Eq. (14), letting [similarly to what is done in [15]]

$$\boldsymbol{m} = -\frac{k_\omega}{\|\boldsymbol{b}\|}\dot{\hat{\boldsymbol{b}}} \tag{15}$$

where the command to the torque rods depends on the time derivative of the unit vector parallel to the magnetic field $\hat{\boldsymbol{b}}$ rather than the time derivative of $\boldsymbol{b}$. Note also that the gain k_ω replaces the sign function used by Markley [15]. Global asymptotic stability to a zero absolute angular rate is no longer attainable by means of the considered theoretical framework. Nonetheless, the absolute angular speed can be reduced down to a value of the same order of magnitude as the orbit rate (that is, 10^{-3} rad/s) as in the case when a standard B-dot command law is used. The residual angular speed is related to the error in estimating the absolute time derivative of the magnetic field from onboard measurement only when no absolute attitude information is available.

Finally, the physical interpretation of the stability proof discussed above for the command law expressed by Eq. (14) leads to a further result, relevant for the practical implementation of the control system. This is discussed in the next subsection, where an optimal value for the control law gain is derived, which allows for a relatively fast convergence toward the rest state for the spacecraft from arbitrary initial conditions.

E. Design of the Gain k_ω

The gain design technique is derived by analyzing the closed-loop dynamics of the component of $\boldsymbol{\omega}$ perpendicular to the Earth magnetic field, $\boldsymbol{\omega}_\perp = (\mathbb{I}_3 - \hat{\boldsymbol{b}}\hat{\boldsymbol{b}}^T)\boldsymbol{\omega}$. The time derivative of $\boldsymbol{\omega}_\perp$ can be expressed as

$$\frac{\mathrm{d}\boldsymbol{\omega}_\perp}{\mathrm{d}t} = (\mathbb{I}_3 - \hat{\boldsymbol{b}}\hat{\boldsymbol{b}}^T)\boldsymbol{I}^{-1}[\boldsymbol{M} - \boldsymbol{\omega} \times (\boldsymbol{I}\boldsymbol{\omega})] - \left[\frac{\mathrm{d}\hat{\boldsymbol{b}}}{\mathrm{d}t}\hat{\boldsymbol{b}}^T + \hat{\boldsymbol{b}}\left(\frac{\mathrm{d}\hat{\boldsymbol{b}}}{\mathrm{d}t}\right)^T\right]\boldsymbol{\omega} \tag{16}$$

The term $\boldsymbol{\omega} \times (\boldsymbol{I}\boldsymbol{\omega})$ is usually small with respect to the others, being a second-order term for $\|\boldsymbol{\omega}\| \ll 1$. Moreover, it is close to $\boldsymbol{0}$ independently of the angular speed for any almost-cubic satellite configuration. The remaining terms are related to the effects of the control torque $\boldsymbol{M}$ and the (relative) motion of the magnetic field $\boldsymbol{b}$ with respect to the body frame $\mathbb{F}_B$ that, in turn, is determined by the motion of $\boldsymbol{b}$ and $\mathbb{F}_B$ with respect to the orbit frame $\mathbb{F}_O$.

As is apparent from Eq. (8), the control torque vanishes whenever $\boldsymbol{\omega}$ becomes parallel to $\boldsymbol{b}$, so this situation needs to be avoided. In such a case, only the slow motion of the magnetic field with respect to $\mathbb{F}_O$ prevents the spacecraft from achieving a gyroscopically stabilized spin motion about $\boldsymbol{b}$, but the resulting convergence toward $\|\boldsymbol{\omega}\| = 0$ would be extremely slow, as shown in the next section. It is thus necessary to prevent the available control torque (perpendicular to $\boldsymbol{b}$) from canceling $\boldsymbol{\omega}_\perp$ when $\|\boldsymbol{\omega}\| \neq 0$. This is possible by requiring that the variation of the norm of $\boldsymbol{\omega}_\perp$ is, at most, as fast as its rotation rate with respect to $\mathbb{F}_B$.

If the gyroscopic coupling term is neglected, substitution of the control law defined by Eq. (8) into Eq. (16) provides the equation

$$\frac{\mathrm{d}\boldsymbol{\omega}_\perp}{\mathrm{d}t} \cong -k_\omega(\mathbb{I}_3 - \hat{\boldsymbol{b}}\hat{\boldsymbol{b}}^T)\boldsymbol{I}^{-1}(\mathbb{I}_3 - \hat{\boldsymbol{b}}\hat{\boldsymbol{b}}^T)\boldsymbol{\omega} - \left[\frac{\mathrm{d}\hat{\boldsymbol{b}}}{\mathrm{d}t}\hat{\boldsymbol{b}}^T + \hat{\boldsymbol{b}}\left(\frac{\mathrm{d}\hat{\boldsymbol{b}}}{\mathrm{d}t}\right)^T\right]\boldsymbol{\omega} \tag{17}$$

where it is possible to introduce the expression of the time derivative of $\hat{\boldsymbol{b}}$, given by

$$\dot{\hat{\boldsymbol{b}}} = \frac{\mathrm{d}}{\mathrm{d}t}(\mathbb{T}_{BO}\hat{\boldsymbol{b}}_O) = \mathbb{T}_{BO}\left(\frac{\mathrm{d}\hat{\boldsymbol{b}}_O}{\mathrm{d}t}\right) - \boldsymbol{\omega}^r \times \hat{\boldsymbol{b}}$$

By means of the coordinate transformation matrix $\mathbb{T}_{BO}$, the term between square parentheses can be recast in the form

$$\left[\frac{\mathrm{d}\hat{\boldsymbol{b}}}{\mathrm{d}t}\hat{\boldsymbol{b}}^T + \hat{\boldsymbol{b}}\left(\frac{\mathrm{d}\hat{\boldsymbol{b}}}{\mathrm{d}t}\right)^T\right] = \mathbb{T}_{BO}\left[\frac{\mathrm{d}\hat{\boldsymbol{b}}_O}{\mathrm{d}t}\hat{\boldsymbol{b}}_O^T + \hat{\boldsymbol{b}}_O\left(\frac{\mathrm{d}\hat{\boldsymbol{b}}_O}{\mathrm{d}t}\right)^T\right]\mathbb{T}_{BO}^T - \tilde{\boldsymbol{\Omega}}^r(\hat{\boldsymbol{b}}\hat{\boldsymbol{b}}^T) + (\hat{\boldsymbol{b}}\hat{\boldsymbol{b}}^T)\tilde{\boldsymbol{\Omega}}^r \tag{18}$$

It is thus possible to obtain a compact formulation

$$\left[\frac{\mathrm{d}\hat{\boldsymbol{b}}}{\mathrm{d}t}\hat{\boldsymbol{b}}^T + \hat{\boldsymbol{b}}\left(\frac{\mathrm{d}\hat{\boldsymbol{b}}}{\mathrm{d}t}\right)^T\right] = \mathbb{T}_{BO}\mathcal{B}\mathbb{T}_{BO}^T - \mathcal{C} \tag{19}$$

where the matrix

$$\mathcal{B} = \frac{1}{\|\boldsymbol{b}_O\|^2}\left[\dot{\boldsymbol{b}}_O\boldsymbol{b}_O^T + \boldsymbol{b}_O\dot{\boldsymbol{b}}_O^T - \frac{2(\dot{\boldsymbol{b}}_O^T\boldsymbol{b}_O)\boldsymbol{b}_O\boldsymbol{b}_O^T}{\|\boldsymbol{b}_O\|^2}\right] \tag{20}$$

can be analytically evaluated from Eq. (5), while $\mathcal{C} = \tilde{\boldsymbol{\Omega}}^r(\hat{\boldsymbol{b}}\hat{\boldsymbol{b}}^T) - (\hat{\boldsymbol{b}}\hat{\boldsymbol{b}}^T)\tilde{\boldsymbol{\Omega}}^r$ depends on the angular velocity $\boldsymbol{\omega}^r$ with respect to the orbit frame $\mathbb{F}_O$. The matrix $\tilde{\boldsymbol{\Omega}}^r$ represents, as usual, the skew-symmetric matrix equivalent of the cross product, such that $\tilde{\boldsymbol{\Omega}}^r\boldsymbol{r} = \boldsymbol{\omega}^r \times \boldsymbol{r}$. Finally, after defining the matrix $\mathcal{A} = (\mathbb{I}_3 - \hat{\boldsymbol{b}}\hat{\boldsymbol{b}}^T)\boldsymbol{I}^{-1}(\mathbb{I}_3 - \hat{\boldsymbol{b}}\hat{\boldsymbol{b}}^T)$, Eq. (16) can be approximated as follows:

$$\frac{\mathrm{d}\boldsymbol{\omega}_\perp}{\mathrm{d}t} \cong -k_\omega\mathcal{A}\boldsymbol{\omega} - \mathbb{T}_{bo}\mathcal{B}\mathbb{T}_{bo}^T\boldsymbol{\omega} + \mathcal{C}\boldsymbol{\omega} \tag{21}$$

The latter equation shows how the time derivative of $\boldsymbol{\omega}_\perp$, after neglecting the gyroscopic coupling terms, is made of three contributions proportional to $\boldsymbol{\omega}$: the first term of the right-hand side, which contains the gain k_ω and is related to the command torque perpendicular to $\hat{\boldsymbol{b}}$, will be referred to as the active control term, directly affecting the magnitude of $\boldsymbol{\omega}_\perp$; the second and the third terms are related to the rotation rate of the Earth magnetic field vector with respect to $\mathbb{F}_B$, thus affecting only the direction of $\boldsymbol{\omega}_\perp$. For this reason, these latter terms will be referred to as the rotational ones.

When high values of k_ω are chosen, the magnitude of the transverse component $\boldsymbol{\omega}_\perp$ rapidly vanishes. This makes the available control moment about the angular velocity vector close to zero once $\boldsymbol{\omega} \approx \omega\hat{\boldsymbol{b}}$. The only possibility to further decrease $\|\boldsymbol{\omega}\|$ thus relies on the residual angle α between $\boldsymbol{b}$ and $\boldsymbol{\omega}$ induced by the rotation of $\boldsymbol{b}$ itself with respect to the rotating orbit frame $\mathbb{F}_O$, which allows for a minimal controllability. For high values of k_ω, α remains very small and the expected behavior of the system in this scenario is a fast transient (where a certain amount of kinetic energy is dissipated by canceling $\boldsymbol{\omega}_\perp$) followed by a very slow convergence, a sort of creeping dissipation during which $\boldsymbol{\omega}$ constantly tracks the direction of $\boldsymbol{b}$. If a smaller value for k_ω is chosen, the angle α becomes wider, thus allowing for a faster detumbling, but if the gain is too small, a slow dynamics is obviously obtained, which again results into longer time intervals for bringing the satellite to rest, thus completing the detumbling.

A reasonable value of k_ω must thus be sought that prevents these two extreme situations. A suitable dynamics for $\boldsymbol{\omega}_\perp$ is obtained by making the order of magnitude of the active term equal to that of the rotational ones in Eq. (21). In this way, after an initial transient during which the dipoles are saturated if $\|\boldsymbol{\omega}\| \gg \Omega$, 1) an excessively fast decrease of $\boldsymbol{\omega}_\perp$ is avoided, which would make the available control power about $\boldsymbol{\omega}$ drop to zero; and 2) a sufficient control power is available most of the time for completing the detumbling in a limited amount of time (in the order of one orbit period) by use of magnetic actuators only. Note that, when the dipoles are saturated, the expected closed-loop behavior matches that obtained from the switching control logic proposed by Markley [15], but when the angular speed becomes smaller, the convergence toward a complete detumbled condition is faster, if the control action is properly modulated.

To enforce the desired condition on the three terms of Eq. (21), one thus needs that

$$\begin{aligned}\mathcal{O}(\|k_\omega\mathcal{A}\boldsymbol{\omega}\|) &= \mathcal{O}(\|\mathbb{T}_{BO}\mathcal{B}\mathbb{T}_{BO}^T\boldsymbol{\omega} - \mathcal{C}\boldsymbol{\omega}\|) \\ &\leq \mathcal{O}(\|\mathbb{T}_{BO}\mathcal{B}\mathbb{T}_{BO}^T\boldsymbol{\omega}\|) + \mathcal{O}(\|\mathcal{C}\boldsymbol{\omega}\|)\end{aligned} \tag{22}$$

With the definition of norm for a linear operator $\boldsymbol{M} \in \mathbb{R}^{n\times n}$ as

$$\|\boldsymbol{M}\| = \max_{\boldsymbol{v}\in\mathbb{R}^n}\left(\frac{\|\boldsymbol{M}\boldsymbol{v}\|}{\|\boldsymbol{v}\|}\right) = \max_{1\leq i\leq n}(|\lambda_i^{\boldsymbol{M}}|)$$

where $\lambda_i^{\boldsymbol{M}}$, $i = 1, 2, \ldots, n$ are the eigenvalues of $\boldsymbol{M}$, the desired condition can be enforced by imposing

$$k_\omega\max_{\boldsymbol{\omega}}\left(\frac{\|\mathcal{A}\boldsymbol{\omega}\|}{\|\boldsymbol{\omega}\|}\right) = \max_{\boldsymbol{\omega}}\left(\frac{\|\mathcal{B}\boldsymbol{\omega}\|}{\|\boldsymbol{\omega}\|}\right) + \max_{\boldsymbol{\omega}}\left(\frac{\|\mathcal{C}\boldsymbol{\omega}\|}{\|\boldsymbol{\omega}\|}\right) \tag{23}$$

where one should note that the presence of the rotation matrix $\mathbb{T}_{BO}$ in the first term of the right-hand side is not relevant, inasmuch as it does not affect the norm of the vectors. The term on the left-hand side is easily obtained from the definition of $\mathcal{A}$, where

$$\max_{\boldsymbol{\omega}}\left(\frac{\|\mathcal{A}\boldsymbol{\omega}\|}{\|\boldsymbol{\omega}\|}\right) = \max(\|\lambda_i^{I^{-1}}\|) = [\min_{k=1,2,3} J_k]^{-1} = \frac{1}{J_{\min}} \tag{24}$$

and where $J_{\min}$ is the minimum moment of inertia.

The first term of the right-hand side is not so easily amenable, but from the definition of $\boldsymbol{b}_O$ and $\dot{\boldsymbol{b}}_O$, it is possible to evaluate $\mathcal{B}$ analytically. Its maximum eigenvalue, determined numerically over one orbit, is reported in Fig. 2 (continuous line). Letting $t_0 = \eta_m/\Omega$,

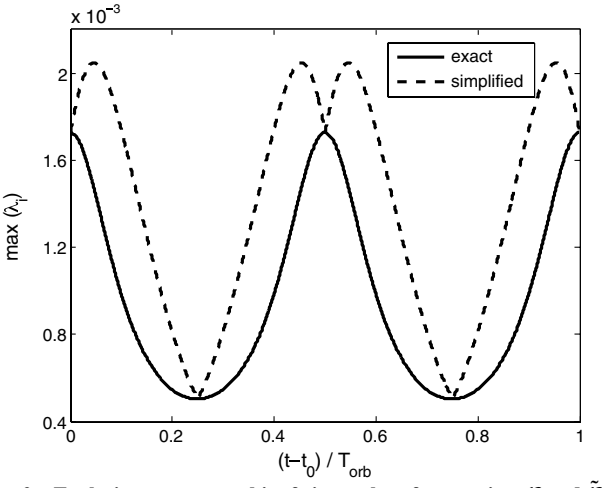

Fig. 2 Evolution over one orbit of eigenvalues for matrices $\mathcal{B}$ and $\tilde{\mathcal{B}}$.

the maximum and minimum values of the maximum eigenvalue are attained alternately at $(t - t_0)/T_{\text{orb}} = k/4, k = 0, 1, 2, 3, 4$, when $\boldsymbol{b}_O$ and $\dot{\boldsymbol{b}}_O$ are mutually perpendicular (that is, $\boldsymbol{b}_O^T \dot{\boldsymbol{b}}_O = 0$). After dropping the term proportional to $\boldsymbol{b}_O^T \dot{\boldsymbol{b}}_O$ in the definition of $\mathcal{B}$, the eigenvalues of the simplified matrix

$$\tilde{\mathcal{B}} = \frac{1}{\|\boldsymbol{b}_O\|^2}[\dot{\boldsymbol{b}}_O \boldsymbol{b}_O^T + \boldsymbol{b}_O \dot{\boldsymbol{b}}_O^T] \tag{25}$$

can be determined analytically and are indicated by the dashed line in Fig. 2. The maximum values of $\|\mathcal{B}\boldsymbol{\omega}\|/\|\boldsymbol{\omega}\|$ over one orbit can thus be evaluated as

$$\max_{t\in[t_0,t_0+T_{\text{orb}}]}\left[\max_{\boldsymbol{\omega}}\left(\frac{\|\mathcal{B}\boldsymbol{\omega}\|}{\|\boldsymbol{\omega}\|}\right)\right] = \left[\max_{\boldsymbol{\omega}}\left(\frac{\|\tilde{\mathcal{B}}\boldsymbol{\omega}\|}{\|\boldsymbol{\omega}\|}\right)\right]_{\Omega t-\eta_m=k\pi} \tag{26}$$

One thus gets

$$\max_{t\in[t_0,t_0+T_{\text{orb}}]}\|\mathcal{B}\| = \|\tilde{\mathcal{B}}\|_{\Omega t-\eta_m=k\pi} = [\max_j(\|\lambda_j^{\tilde{\mathcal{B}}}\|)]_{\Omega t-\eta_m=k\pi}$$
$$= 2\Omega \sin\xi_m \tag{27}$$

As for the last term, noting that 1) $\|\hat{\boldsymbol{b}}\hat{\boldsymbol{b}}^T\| = 1$ if $\hat{\boldsymbol{b}}$ is a unit vector, 2) $\|\tilde{\boldsymbol{\Omega}}^r\| = \|\boldsymbol{\omega}^r\|$ if $\tilde{\boldsymbol{\Omega}}^r$ is the skew-symmetric matrix equivalent of the cross product, and that 3) for any pair of linear operators $\boldsymbol{A}$ and $\boldsymbol{B}$, $\|\boldsymbol{AB}\| \le \|\boldsymbol{A}\|\|\boldsymbol{B}\|$, the following inequality can be easily derived from the definition of $\mathcal{C}$:

$$\max_{\boldsymbol{\omega}}\left(\frac{\|\mathcal{C}\boldsymbol{\omega}\|}{\|\boldsymbol{\omega}\|}\right) \le 2\|\boldsymbol{\omega}^r\| \tag{28}$$

Focusing the attention on the last part of the detumbling maneuver, when the absolute angular velocity of the spacecraft drops close to zero, the angular velocity relative to the orbit frame $\mathbb{F}_O$ becomes approximately Ω in magnitude, so that a value around

$$\max_{\boldsymbol{\omega}}\left(\frac{\|\mathcal{C}\boldsymbol{\omega}\|}{\|\boldsymbol{\omega}\|}\right) \approx 2\Omega \tag{29}$$

is expected, as explained also in [6].

Summing up the results reported in Eqs. (24), (27), and (29), one can estimate a reasonable value for k_ω choosing

$$k_\omega = 2\Omega(1 + \sin\xi_m)J_{\min} \tag{30}$$

IV. Results and Discussion

A. Numerical Simulations

The control law described in the previous section is applied to the detumbling maneuver for a LEO microsatellite equipped with three mutually orthogonal magnetic coils. A maximum magnetic dipole moment $m_{\max} = 2\ \text{A}\cdot\text{m}^2$ is assumed for each torque rod. Other spacecraft data and parameters relevant for the proposed application

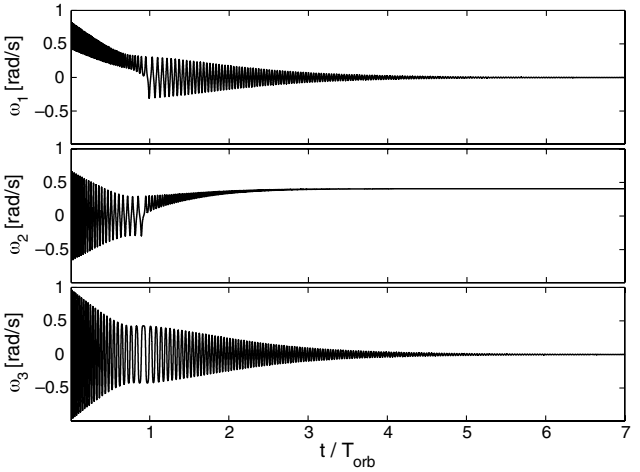

Fig. 3 Evolution of angular velocity components for $\boldsymbol{b} = (0, -1, 0)^T$.

are reported in Table 1, together with the initial conditions for three example maneuvers (cases A, B, and C). Numerical simulations facilitate validation of the results derived in the previous sections and their physical interpretation for the nominal value of the control law gain k_ω obtained from Eq. (30).

In case A, the orbit plane coincides initially with the geomagnetic equatorial plane, so that $\boldsymbol{b}$ lies along the normal to the orbit plane at time $t = 0$, when $\hat{\boldsymbol{b}}_O = (0, -1, 0)^T$. In case A*, the same initial conditions of case A are used, but the rotation of the geomagnetic field, fixed to the Earth, is neglected. For $\Omega = 0$, $\hat{\boldsymbol{b}}_O$ remains constant in $\mathbb{F}_O$. Such a case does not correspond to a realistic situation, but it is useful to prove that the detumbling cannot be completed because of the presence of equilibria (other than the origin) on the isosurfaces $V = \mathcal{T} =$ constant. As shown in Fig. 3, the spacecraft achieves a pure spin condition about its principal axes of maximum inertia ($\hat{\boldsymbol{e}}_2$ for the considered case). This occurs because the magnetic actuators cannot deliver a control torque about the (inertially fixed) direction of the magnetic field and, consequently, the component of the angular momentum vector along $\hat{\boldsymbol{b}}$ remains constant. The asymptotic value of the angular speed (0.41 rad/s for case A^*) can be evaluated from the limit value of $J_i\omega_i = \hat{\boldsymbol{b}}^T(\boldsymbol{I}\boldsymbol{\omega}_0)$, where J_i is the maximum principal moment of inertia. A minimum energy condition is thus reached when the spacecraft spins about $\hat{\boldsymbol{e}}_i$ ($i = 2$ in case A*).

A different process takes place in a more realistic scenario, where the rotation of the geomagnetic equatorial plane slowly varies the inclination ξ_m of the orbit plane with respect to the geomagnetic equator. The aperture of the elliptic cone described by $\boldsymbol{b}$ in $\mathbb{F}_O$ increases, and a nonzero average control power becomes available about all the axes of the orbit frame. This allows the completion of the detumbling, although more than five orbits are necessary to complete the maneuver (dashed line in Fig. 4). A faster convergence is obtained, if ξ_m never vanishes, as for case B, with $i = 65$ deg and $54 < \xi_m < 76$ deg. In this third case, the motion starting from a value

Table 1 Spacecraft and orbit data, with initial conditions for cases A, B, and C

Parameter	Symbol	Value	Units
	Spacecraft and orbit data		
Principal moments of inertia	J_1, J_2, J_3	0.33, 0.37, 0.35	$\text{kg}\cdot\text{m}^2$
Maximum magnetic dipole	$m_{\max}$	2.0	$\text{A}\cdot\text{m}^2$
Orbit radius	r_c	7021	km
Orbit period	T_{orb}	5855	s
Geomagnetic tilt angle	γ_m	11.44	deg
Inclination: case A	i	11	deg
Cases B and C		65	
	Initial conditions		
Cases A and B	$\boldsymbol{\omega}_0$	$(0.604, -0.760, -0.384)^T$	rad/s
	$\mathbf{Q}_0$	$(-0.062, 0.925, -0.007, 0.375)^T$	
Case C	$\boldsymbol{\omega}_0$	$(1.0, 0.0, 0.0)^T$	rad/s
	$\mathbf{Q}_0$	$(0.525, -0.514, 0.206, 0.646)^T$	

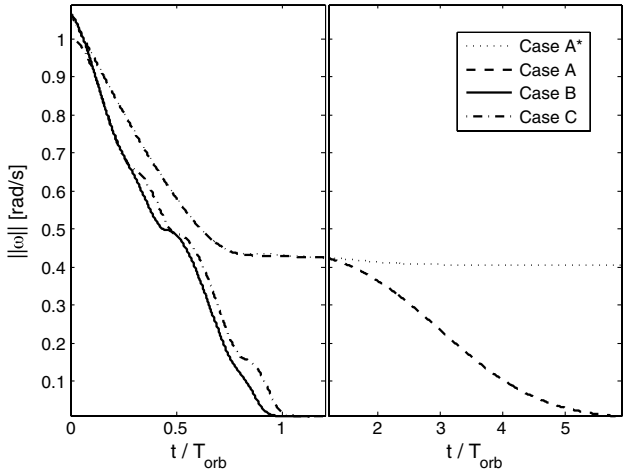

Fig. 4 Evolution of $\|\boldsymbol{\omega}\|$ for cases A (dashed line), B (continuous), and C (dashed–dotted).

of $\|\boldsymbol{\omega}\| \approx 1$ rad/s is stopped in little more than one orbit (solid plot in Fig. 4).

To fully assess the performance of the control law, the unwanted situation in which the spacecraft spins around one of its principal axes of inertia perfectly aligned with the magnetic field vector is assumed as the initial condition for case C. Also in this case, the angular velocity is driven toward 0, although initially it does not change (a horizontal tangent being clearly visible at $t = 0$ for the dashed–dotted line in Fig. 4), that represents the evolution of $\|\boldsymbol{\omega}\|$ for case C. As a consequence of this initial condition, the convergence time is slightly longer; however, the difference is insignificant for this particular case.

During the initial transient, when the angular velocity is not changed because no control power is available about the spin axis, the magnetic field rotates, and as soon as the angle α between $\boldsymbol{\omega}$ and $\boldsymbol{b}$ achieves a sizable value, the control law is capable of starting its action, decreasing $\|\boldsymbol{\omega}\|$ toward 0. The physical interpretation of this phenomenon in terms of angular displacement between the angular velocity and magnetic field vector is confirmed by Fig. 5, where the evolution of α for the four cases is shown. It is evident how, in case A^*, α approaches π rad in less than one orbit and, consequently, $\boldsymbol{\omega}$ and $\boldsymbol{b}$ become parallel and no control torque can then be produced to decrease the angular velocity further. In contrast, when the magnetic field vector rotates with respect to the orbit frame (cases A, B, and C), a nonzero value of α is present most of the time during the final phase of the detumbling, allowing delivery of a nonzero control action. In case A, it is necessary to wait a few orbits, during which time the geomagnetic equator rotates away from the orbit plane, thus making $\xi \neq 0$.

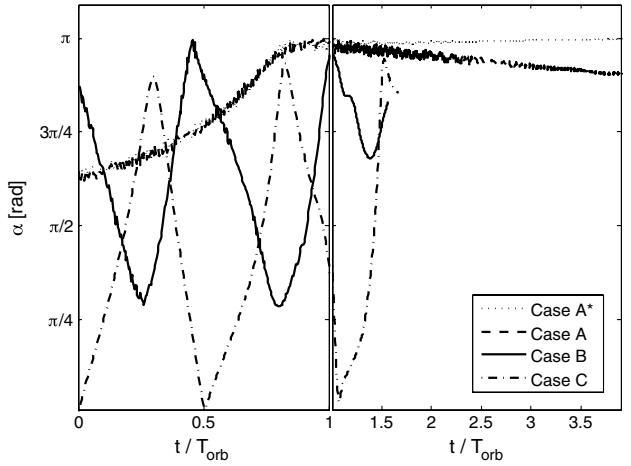

Fig. 5 Evolution of α for cases A (dashed line), B (continuous), and C (dashed–dotted).

Finally, Fig. 6 shows a comparison among the time histories of angular rates obtained for three different detumbling laws: 1) dipole moments expressed as in Eq. (14); 2) standard B-dot command law, $\boldsymbol{m} = -K_{\dot{\boldsymbol{b}}}\dot{\boldsymbol{b}}$ taken from [6]; and 3) modified B-dot, expressed by Eq. (15). To provide a fair comparison, the gain for the standard B-dot command law was chosen according to the analysis performed in the previous section by letting $K_{\dot{\boldsymbol{b}}} = \bar{k}_\omega / \|\dot{\boldsymbol{b}}\|^2$. Absolute angular rates are represented in Fig. 6 by thick lines, whereas angular speed with respect to the orbit frame $\mathbb{F}_O$ is shown by thin lines.

The initial deceleration transient is identical for the three command laws, as magnetic coils saturate. Differences are visible in the final part (enlarged in the bottom part of the plot), where the nominal command law allows for asymptotic convergence to zero absolute angular rate, as predicted by the stability analysis, at the cost of availability of exact information on angular rates. A limit cycle featuring two oscillations per orbit is reached by both B-dot command laws, where the residual absolute angular rate is, on the average, twice the orbit rate. The average residual angular speed relative to $\mathbb{F}_O$ is equal to the orbit rate, as pointed out in [6]. Note that the modified version allows for a faster convergence to the final limit cycle.

B. Monte Carlo Analysis of Detumbling Maneuvers for Different Values of k_ω

The duration of the detumbling maneuver depends on the internal dipole saturation level $m_{\max}$ and on the gain k_ω. The value of $m_{\max}$ is a characteristic of the control hardware and it determines the average rate of variation of $\|\boldsymbol{\omega}\|$ during the initial phase of the detumbling, when magnetic coils are saturated, whereas k_ω governs the final asymptotic convergence toward $\|\boldsymbol{\omega}\| = 0$. It is thus important to prove that the choice derived from Eq. (30) for k_ω is satisfactory in every possible operating condition. In this respect, the tumbling motion after the payload is ejected from the upper stage of the rocket launcher is (at least partially) random. Nonetheless, adequate performance of the detumbling process is mandatory, whatever may be the tumbling motion experienced by the spacecraft and the random attitude at which detumbling starts [16]. At the same time, it is well known that, when a Lyapunov-like approach is invoked to develop a feedback control law, elegant stability proofs are often derived, but an estimate of performance is usually not available and the time required to converge to the desired state can become unpredictably large. The Monte Carlo analysis addresses both these aspects.

Eight random numbers are generated with uniform distribution between a maximum and a minimum value: three for the angular rates, with $\|\boldsymbol{\omega}_0\| \approx 1$ rad/s; three for the vector part of the quaternion, with $\|\boldsymbol{q}_0\| \leq 1$ and $\bar{q}_0 = (1 - \boldsymbol{q}_0^T \boldsymbol{q}_0)^{1/2}$; one for β_m, between $-\pi$ and π; and one for the initial phase along the orbit,

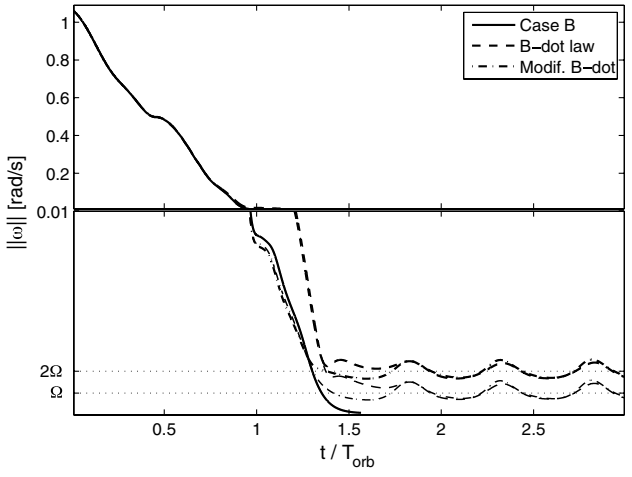

Fig. 6 Comparison with classical B-dot control law (thick lines: absolute angular speed; thin lines: angular speed relative to $\mathbb{F}_O$; Modif. denotes modified).

$t_0 \in [-T_{\text{orb}}/2; T_{\text{orb}}/2]$. Note that the angular rates are scaled in order that all the simulations start from the same magnitude of the angular momentum, $\|\boldsymbol{h}_0\| = 0.37$ kg m^2/s.

As a last practical issue, an estimate of the maneuver cost is provided in terms of electrical power consumption. This is relevant to properly size the batteries required to perform detumbling, a suboptimal performance in terms of convergence time being acceptable if it results in a smaller weight for the required battery system. The magnetic dipole moment is proportional to the current absorbed. The total electrical energy $\mathcal{E}$ necessary for completing the detumbling is thus proportional to

$$\mathcal{E} \propto E = \int_0^{t_F} \left(\sum_{i=1}^{3} |m_i| \right) \mathrm{d}t$$

Figure 7 shows the results obtained from the Monte Carlo analysis, performed over 1000 test cases, where performance in terms of time (Fig. 7a) and electrical energy (Fig. 7b) are shown for different values of the gain k_ω. The dashed line labeled t_{95} indicates the average number of orbits necessary for reducing the initial angular rate $\|\boldsymbol{\omega}\| \approx 1$ rad/s by 95%, while the solid one indicates the average number of orbits t_F necessary for stopping the tumbling motion completely. Given the asymptotic nature of the convergence, a value of 99.99% was chosen as the threshold for a sufficiently slow residual motion, with $\|\boldsymbol{\omega}\| < 10^{-4}$ rad/s. The candle bars indicate the standard deviation over the considered set of tests.

Performance for the nominal value of the gain is obtained for $k_\omega/\bar{k}_\omega = 1$. Note that, with increase in the gain, a longer average convergence time t_F is obtained, whereas a minor sensitivity of t_{95} to the control gain is apparent for $k_\omega > \bar{k}_\omega$. Given the high value of the initial angular velocity, all the torque rods are at saturation during the initial phase of the detumbling and $\|\boldsymbol{\omega}\|$ decreases almost linearly with time. This initial transient is followed by an almost exponential decrease of the angular rate only if k_ω is sufficiently small. If $k_\omega > \bar{k}_\omega$, the magnetic actuators remain saturated for a longer time and the angular rate component perpendicular to $\boldsymbol{b}$ is almost canceled when the component parallel to $\boldsymbol{b}$ is still in the order of 0.1 rad/s. At this point, 90% of the initial angular momentum has been dumped, but only a small control action remains available for further reducing its magnitude because $\boldsymbol{\omega}$ is tracking the direction of $\boldsymbol{b}$ and the resulting value of $\boldsymbol{M}$ is close to 0. This causes t_F to be significantly higher, but t_{95} is less sensitive to the value of the gain because it depends mainly on the initial rate of variation of $\|\boldsymbol{\omega}\|$, determined by $m_{\max}$.

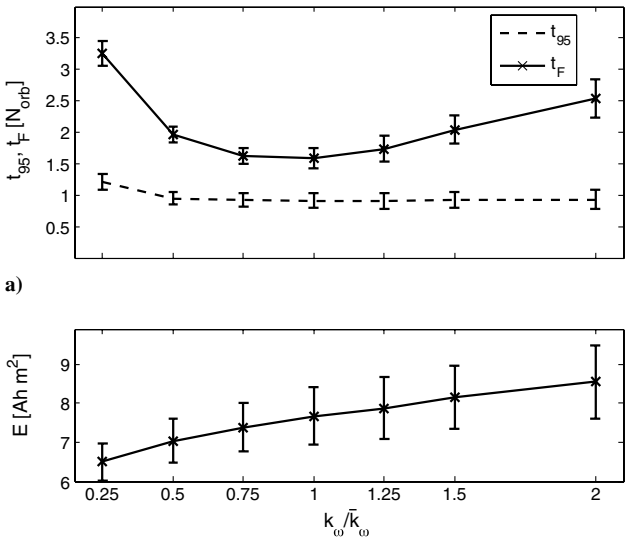

Fig. 7 Performance analysis in terms of a) average detumbling time and b) electrical energy consumption.

On the other hand, a small value of the gain does not allow full use of the available control power in the transverse direction, so again, longer convergence times result. The best average performances in terms of both t_{95} and t_F are obtained for $\bar{k}_\omega$, although the difference with respect to the case $k_\omega = 0.75\bar{k}_\omega$ is marginal. The actual optimal value is thus expected to lie between these two values. It is noteworthy that, in spite of considerable simplifications involved for derivation of Eq. (30), it provides a reliable value of the gain in terms of a few relevant system parameters and results in a quasi-optimal performance.

An equally important aspect is related to the distribution of the results. Higher values of the standard deviation, indicated by candle bars in Fig. 7a, are typical of tests run with higher values of k_ω, indicating that a large number of admissible initial conditions require a significantly longer convergence time with respect to the average value. The standard deviation achieves smaller values for $k_\omega < \bar{k}_\omega$.

A reduction of the gain with respect to the nominal value $\bar{k}_\omega$ offers an interesting property when the energy consumption parameter (reported in Fig. 7b) is considered. A clear trend is again visible, where both the average value of the energy required for completing the detumbling and its standard deviation steadily grow with k_ω. In this respect, smaller values of the gain allow for completing the detumbling with less electrical power expenditure. However, the savings in terms of total power expenditure appear rather marginal (approximately 20% for the smallest considered value of k_ω with respect to the nominal case); if compared with the penalty paid in terms of convergence time, that almost doubles.

The peak of the electrical power absorbed $\mathcal{P}_{\max}$ is always 6.0 A m^2 during the initial phase of detumbling, when torque rods are saturated. Obviously, a more powerful set of magnetic torquers would result in faster detumbling, at the cost of an increased weight of the system and higher overall electrical power expenditure. A reduction of the gain, which does not saturate the magnetic actuators or saturates them for a shorter time, becomes interesting if slower detumbling is acceptable for the considered mission scenario. An engineering tradeoff is clearly present that can be analyzed by means of the approach adopted here, starting from a physically meaningful first guess for the control law gain.

As a final comment on the practical application of the proposed control law, it should be noted that, during detumbling, the spacecraft cannot perform its mission tasks, as pointing accuracy remains degraded during this period. On one hand, this clearly highlights the importance of minimizing the time necessary to detumble the satellite, thus proving the relevance of an optimal value of k_ω. On the other hand, magnetic actuators are characterized by a limited control power, compared with thruster-based ACS. This results in longer settling times. In the present case, settling times obtained from the test cases are also particularly long because of the high value of the initial angular speed.

V. Conclusions

A rigorous proof of convergence for a B-dot-like control law is derived by means of a new corollary to Barbalat's lemma. The physical interpretation of the control law allows for a preliminary definition of the gain k_ω. A nominal value for k_ω is obtained, which prevents the angular speed vector from becoming parallel to the Earth's magnetic field $\boldsymbol{b}$. Consequently, the available control torque does not drop close to zero and a faster detumbling is obtained.

This interpretation of the control law is confirmed with the simulation of four detumbling examples. To test the control approach, a thorough Monte Carlo analysis is also performed for 1000 detumbling cases, demonstrating that good performances (on average) are obtained for values of the control gain close to the nominal one. The positive effects in terms of electrical power expenditure of smaller gains for the control law suggest choosing gains in the range between the nominal value and its half.

Acknowledgments

The authors express their gratitude to the anonymous reviewers and the Associate Editor who allowed for improving the paper throughout the revision process.

References

[1] Wertz, J., *Spacecraft Attitude Determination and Control*, Kluwer, Dordrecht, The Netherlands, 1978, Ch. 19.

[2] Wie, B., *Space Vehicle Dynamics and Control*, AIAA, Reston, VA, 1998, Ch. 7.

[3] Aghili, F., "Time-Optimal Detumbling Control of Spacecraft," *Journal of Guidance, Control, and Dynamics*, Vol. 32, No. 5, Sept.–Oct. 2009, pp. 1671–1675. doi:10.2514/1.43189

[4] Romano, M., "Detumbling and Nutation Canceling Maneuvers With Complete Analytic Reduction For Axially Symmetric Spacecraft," *Acta Astronautica*, Vol. 66, Nos. 7–8, April–May 2010, pp. 989–998. doi:10.1016/j.actaastro.2009.09.015

[5] Coverstone-Carroll, V., "Detumbling and Reorienting Underactuated Rigid Spacecraft," *Journal of Guidance, Control, and Dynamics*, Vol. 19, No. 3, May–June 1996, pp. 708–710. doi:10.2514/3.21680

[6] Stickler, A. C., and Alfriend, K., "Elementary Magnetic Attitude Control System," *Journal of Spacecraft and Rockets*, Vol. 13, No. 5, Sept.–Oct. 1976, pp. 282–287. doi:10.2514/3.57089

[7] Sidi, M. J., *Spacecraft Dynamics and Control: A Practical Engineering Approach*, Cambridge Univ. Press, Cambridge, England, U.K., 1997, Ch. 9.

[8] John S. White, Fred H., and Shlgemoto, K. B., "Satellite Attitude Control Utilizing the Earth's Megnetic Field," NASA TN D-1068, Ames Research Center, Moffett Field, CA, 1961.

[9] Grassi, M., and Pastena, M., "Minimum Power Optimum Control of Microsatellite Attitude Dynamics," *Journal of Guidance, Control, and Dynamics*, Vol. 23, No. 5, Sept.–Oct. 2000, pp. 798–804. doi:10.2514/2.4640

[10] Lovera, M., and Astolfi, A., "Spacecraft Attitude Control Using Magnetic Actuators," *Automatica*, Vol. 40, No. 8, 2004, pp. 1405–1414. doi:10.1016/j.automatica.2004.02.022

[11] Lovera, M., and Astolfi, A., "Global Magnetic Attitude Control of Inertially Pointing Spacecraft," *Journal of Guidance, Control, and Dynamics*, Vol. 28, No. 5, 2005, pp. 1065–1072. doi:10.2514/1.11844

[12] Slotine, J. J. E., and Li, W., *Applied Nonlinear Control*, Prentice–Hall, Upper Saddle River, NJ, 1991, Ch. 4.

[13] Flatley, T., Morgenstern, W., Reth, A., and Bauer, F., "A B-Dot Acquisition Controller for the RADARSAT Spacecraft," *Flight Mechanics Symposium*, edited by D. M. Walls, NASA Goddard Space Flight Center, Greenbelt, MD, May 1997, pp. 79–89.

[14] Hablani, H., "Comparative Stability Analysis and Performance of Magnetic Controllers for Bias Momentum Satellites," *Journal of Guidance, Control, and Dynamics*, Vol. 18, No. 6, 1995, pp. 1313–1320. doi:10.2514/3.21547

[15] Markley, F. L., "Attitude Control Algorithms for the Solar Maximum Mission," Guidance and Control Conference, Paolo Alto, CA, AIAA Paper 1978-1247, Aug. 1978, pp. 59–69.

[16] Fabbri, V., Giulietti, F., Tortora, P., Barbagallo, D., and Gabrielli, A., "Development of a Payload Dispersion and Contamination Analysis Tool for the Vega Maiden Flight," *4th International Conference on Astrodynamics Tools and Techniques* [CD-ROM], Madrid, ESA, Noordwijk, The Netherlands, May 2010.